JOURNAL OF RAMAN SPECTROSCOPY
J. Raman Spectrosc. 2007; **38**: 551–558
Published online 21 December 2006 in Wiley InterScience
(www.interscience.wiley.com) DOI: 10.1002/jrs.1680

JRS

Raman and *ab initio* study of the conformational isomerism in the 1-ethyl-3-methyl-imidazolium bis(trifluoromethanesulfonyl)imide ionic liquid

J. C. Lassègues,[1]* J. Grondin,[1] R. Holomb[2,3] and P. Johansson[2]

[1] Laboratoire de Physico-Chimie Moléculaire, UMR 5803, CNRS, Université Bordeaux I, 351 Cours de la Libération, 33405 Talence Cedex, France
[2] Department of Applied Physics, Chalmers University of Technology, SE-41296, Göteborg, Sweden
[3] Department of Solid State Electronics, Uzhhorod National University, Uzhhorod, Ukraine

Received 5 October 2006; Accepted 19 November 2006

The calculated and experimental Raman spectra of the (EMI^+)$TFSI^-$ ionic liquid, where EMI^+ is the 1-ethyl-3-methylimidazolium cation and $TFSI^-$ the bis(trifluoromethanesulfonyl)imide anion, have been investigated for a better understanding of the EMI^+ and $TFSI^-$ conformational isomerism as a function of temperature. Characteristic Raman lines of the planar (p) and non-planar (np) EMI^+ conformers are identified using the reference (EMI^+)Br^- salt. The anion conformer of C_2 symmetry is confirmed to be more stable than the *cis* (C_1) one by 4.5 ± 0.2 kJ mol^{-1}. At room temperature, the population of *trans* (C_2) anions and np cations is $75 \pm 2\%$ and $87 \pm 4\%$, respectively. Fast cooling quenches a metastable glassy phase composed of mainly C_2 anion conformers and p cation conformers, whereas slow cooling gives a crystalline phase composed of C_1 anion conformers and of np cation conformers. Copyright © 2006 John Wiley & Sons, Ltd.

KEYWORDS: ionic liquid; conformation; Raman spectroscopy; 1-ethyl-3-methylimidazolium; bis(trifluoromethanesulfonyl)imide

INTRODUCTION

The (EMI^+)$TFSI^-$ ionic liquid, where EMI^+ is the 1-ethyl-3-methylimidazolium cation and $TFSI^-$ the bis(trifluoromethanesulfonyl)imide anion, has recently been investigated using Raman spectroscopy and DFT calculations to characterize the conformational states of the cation[1] and the anion.[2] A number of papers have also been devoted either to other properties of this ionic liquid,[3–5] or to the conformational dynamics of the $TFSI^-$ anion in a variety of situations.[6–9] Further theoretical and experimental studies deal with the modelling of ionic liquid salts in which EMI^+ is associated with other anions than $TFSI^-$.[10–16]

In the present work, the DFT calculations of the cation and anion are revisited and additional Raman results on the (EMI^+)$TFSI^-$ system are presented for a better understanding of EMI^+ and $TFSI^-$ conformational isomerism as a function of temperature. Raman spectra of (EMI^+)Br^- are also recorded for comparison, as the crystal structure of this salt has been determined.[10]

*Correspondence to: J. C. Lassègues, Laboratoire de Physico-Chimie Moléculaire, UMR 5803, CNRS, Université Bordeaux I, 351 Cours de la Libération, 33405 Talence Cedex, France. E-mail: jc.lassegues@lpcm.u-bordeaux1.fr

EXPERIMENTAL

The ionic liquids (EMI^+)$TFSI^-$ (99+%) and (EMI^+)Br^- (99+%) were purchased from Solvionic.[17] They are claimed to have melting temperatures of 257 and 326 K, respectively,[17] but they can very easily be obtained in a supercooled liquid state. A solution of 1 mol LiTFSI (Sigma-Aldrich 99.99%) in 40 mol H_2O was also prepared. All these samples were sealed under vacuum in glass tubes for the Raman measurements. The Raman spectra were recorded, as previously described,[8] with a Labram HR800 Jobin-Yvon spectrometer equipped with a krypton ion laser (752.45 nm), an air-cooled CCD detector (ANDOR) and a 600 grooves mm^{-1} grating giving a spectral resolution of 2 cm^{-1}.

First-principles calculations of minimum energy geometry, symmetry and vibrational properties of the planar (p) and non-planar (np) conformers of EMI^+ and of the *cis* (C_1) and *trans* (C_2) conformers of $TFSI^-$ have been carried out using the Gaussian03 quantum-chemical package.[18] Initially, the models were geometry-optimized by the HF/6-311 + G* method and the subsequent calculations of geometry and vibrational spectra were performed using the hybrid (HF + DFT) B3LYP functional consisting of a linear combination of the pure corrected exchange functional proposed by Becke and the

tri-parameter gradient-corrected correlation functional proposed by Lee, Yang and Parr[19–21] and the same basis set (6-311+G*).

RESULTS

DFT calculations

DFT calculations of the IR and Raman spectra of $TFSI^-$ have previously been reported to distinguish spectroscopically the two conformers of this anion in various complexes, salts and solutions.[8,9] More recently, Fujii *et al*.[2] have also reported detailed calculations to study the conformational isomerism of $TFSI^-$ in the $(EMI^+)TFSI^-$ ionic liquid. Using the B3LYP level of theory and 6-31G(d), 6-311+ G(d) and 6-311+G(3df) basis sets, these authors have found scaling factors of 1.019, 1.043 and 1.013, respectively. They have finally preferred the B3LYP/6-311 + G(3df) calculation. For the EMI^+ cation, Umebayashi *et al*.[1] have also used various levels of theory and several basis sets. They chose the MP2/aug-cc-pVDZ calculation because it gave the best prediction for the entire spectrum (scaling factor 0.995). Our DFT calculation of the IR and Raman spectra of EMI^+ are reported in Table 1. In the following, the results of our B3LYP/6-311G* calculations for $TFSI^-$ and EMI^+ are used and compared with the literature results.

Raman study

The Raman spectra of the $(EMI^+)TFSI^-$ and $(EMI^+)Br^-$ ionic liquids and of a LiTFSI aqueous solution (1 : 40) are reported in Fig. 1. The EMI^+ and $TFSI^-$ Raman lines in $(EMI^+)TFSI^-$ are easily identified by comparison with the $(EMI^+)Br^-$ spectrum, which involves only the EMI^+ vibrations, and with the LiTFSI/H_2O spectrum dominated by $TFSI^-$ lines. Vibrational assignments of EMI^+ and $TFSI^-$ have been discussed previously.[1,2,7–9] The spectroscopic distinction between the two conformers of the cation and the anion is a more difficult task. Using the results of Fig. 1, we have first considered spectral regions to which either the cation or the anion alone contributes. Then, from the DFT calculations, we have selected vibrations that produce measurable conformational splittings. According to these criteria, several spectral regions are successively analysed.

The 260–360 cm^{-1} region

The 260–360 cm^{-1} Raman region has previously been shown to be particularly adequate for a conformational analysis of the anion.[8,9] In addition, the EMI^+ contribution to this spectral range consists in a negligibly weak band near 300 cm^{-1} (Fig. 1). The Raman spectra of the $TFSI^-$ conformers calculated by us[8] and by Fujii *et al*.[2] are compared in Fig. 2 with the experimental spectra of $(EMI^+)TFSI^-$ at different temperatures. The two DFT calculations are in reasonably good agreement and predict six vibrations for the C_1 conformer and four vibrations for the C_2 conformer (Fig. 2(a), (b)). However, some of these components merge into broad

Table 1. Calculated IR and Raman spectra of the planar and non-planar EMI^+ conformers

ω, cm^{-1}		I^{IR}_{calc}, km mol^{-1}		I^{Raman}_{calc}, Å^4 a.m.u^{-1}.	
Planar	Non-planar	Planar	Non-planar	Planar	Non-planar
30.9	47.0	0.4	0.3	0.9	1.0
71.2	75.5	0.2	0.1	0.2	0.2
168.6	134.8	3.7	1.3	0.8	1.7
187.3	208	0.5	0.2	0.4	0.1
247.5	231.3	0.6	1.9	1.0	1.0
304.8	291.5	0.2	0.2	0.1	0.3
355.4	377.9	0.5	0.4	0.4	1.7
446.8	425.4	1.0	0.4	4.0	1.2
591.2	592.5	1.3	2.3	6.2	6.2
631.7	632.6	2.9	10.8	0.1	0.2
635.1	660.2	19.5	15.2	0.0	0.2
706.7	699.3	7.5	9.9	2.6	2.6
746.9	744.4	30.3	27.9	0.2	0.2
806.7	802.7	5.0	1.4	0.1	0.1
834.0	824.2	36	39.5	0.3	0.3
870.4	869.1	0.1	0.0	0.5	0.7
976.6	964.7	2.1	3.4	3.0	5.9
1038.1	1037.6	1.2	0.5	5.8	7.7
1049.2	1044.5	0.5	1.0	4.7	3.3
1103.7	1103.7	3.7	3.2	5.7	4.3
1110.5	1107.7	0.6	2.5	3.7	2.9
1129.0	1127.6	12.4	9.4	2.5	1.9
1157.6	1141.7	0.1	3.0	0.8	2.3
1171.2	1158.5	1.7	0.0	0.1	0.6
1173.0	1179.2	106.4	112.8	2.4	1.5
1287.7	1276.0	9.3	0.1	0.7	2.7
1329.0	1317.4	9.1	0.4	12.0	1.5
1334.5	1346.7	2.1	9.6	6.1	28.8
1363.9	1391.4	26.5	11.8	18.8	0.7
1412.1	1414.7	2.4	5.7	13.6	19.0
1430.5	1437.4	9.4	6.3	9.2	3.2
1447.8	1442.5	14.0	3.5	12.7	19.6
1472.1	1469.4	3.3	8.6	6.2	7.8
1498.5	1497.9	17.0	15.9	8.6	8.9
1512.3	1502.9	6.0	10.2	15.2	15.8
1515.2	1508.9	15.3	17.6	10.0	9.3
1521.3	1521.1	2.1	17.6	1.0	1.9
1521.7	1521.6	9.9	7.4	16.0	12.8
1605.8	1599.8	62.8	55.8	1.8	2.5
1611.7	1608.6	16.9	30.2	4.6	3.8
3048.4	3052.4	4.8	4.3	145.8	147.3
3077.4	3078.2	3.2	5.2	162.2	164.1
3077.9	3086.9	8.1	6.9	97.6	84.6
3106.8	3114.8	2.8	3.3	83.9	76.7
3127.6	3126.9	4.8	8.8	102.8	96.8
3129.7	3140.2	11.5	11.0	13.8	11.4
3158.7	3159.2	0.9	0.8	63.7	63.2
3172.4	3173.1	1.1	1.1	44.6	45.5
3277.1	3277.8	12.4	12.3	43.3	40.4
3293.5	3284.9	18.3	25.6	67.0	20.9
3302.5	3295.3	12.9	5.1	61.6	107.6

DOI: 10.1002/jrs

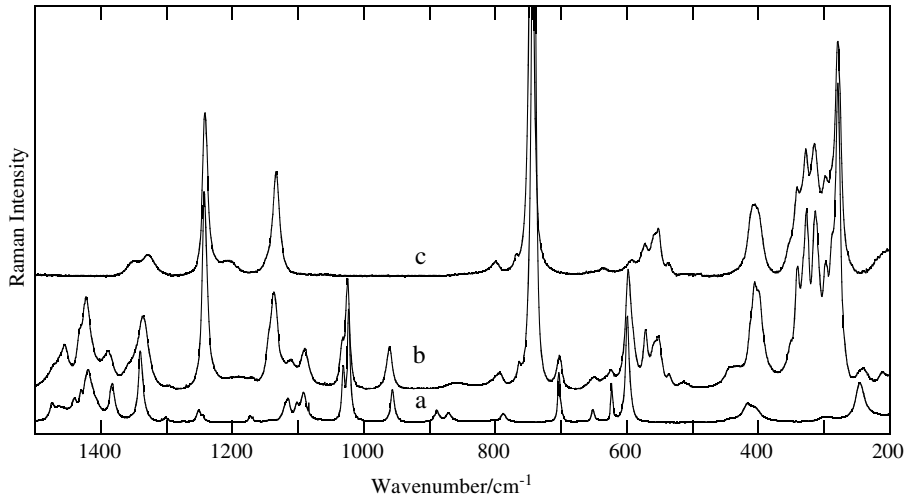

Figure 1. Raman spectra of the ionic liquids (EMI^+)Br^- at 358 K (a); (EMI^+)$TFSI^-$ at 343 K (b); and an aqueous solution of LiTFSI at 298 K (c). The background of water is not subtracted from (c) because it is negligibly weak.

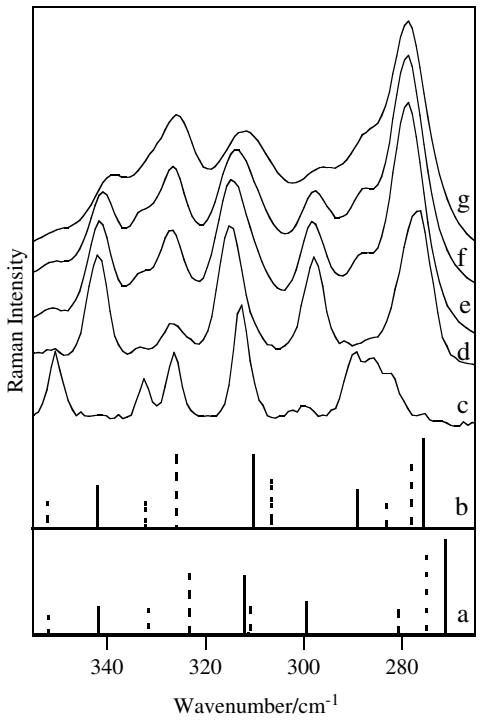

Figure 2. Calculated Raman spectra for the C_2 (solid line) and C_1 (dotted line) conformers of $TFSI^-$: according to Ref. 2 with a scaling factor of 1.032 (a); according to Ref. 8 with a scaling factor of 1.051 (b); experimental spectra of (EMI^+)$TFSI^-$ in the solid state at 113 K after slow cooling (~1 K min^{-1}) (c); in a glassy metastable phase at 113 K after fast cooling (~20 K min^{-1}) (d); in the ionic liquid state at 248 K (e); 298 K (f); and 408 K (g). The scaling factors have been arbitrarily chosen to obtain coincidence with the C_2 peak observed at 341.7 cm^{-1} (d). At 248 K, (EMI^+)$TFSI^-$ is in a supercooled liquid state.

bands in the liquid state. By cooling the (EMI^+)$TFSI^-$ ionic liquid below its solidification temperature, one can hope to displace the conformational equilibria towards a unique anionic or cationic form and to facilitate the comparison with the calculated spectra. Actually, slow cooling (~1 K min^{-1}) produces a thermodynamically stable phase in which the anion adopts the C_1 conformation (Fig. 2(c)), whereas fast cooling (~20 K min^{-1}) quenches the anion in its C_2 conformation with only a small amount of C_1 (Fig. 2(d)). Although the two calculations may present wavenumber differences of up to 10 cm^{-1} for a given line, a one-to-one correspondence with the experimental bands or shoulders can be made unambiguously. Some features remain better separated than others; for example, the C_1 conformer is well characterized by a doublet at 332 and 326 cm^{-1} in the solid phase (Fig. 2(c)), which broadens but is maintained in the liquid state without any interference from the C_2 conformer. This C_2 conformer can be well identified by a separated band at 341.7 cm^{-1} and another at 297 cm^{-1} (Fig. 2(d)). These qualitative observations are corroborated by a fitting of the liquid state spectra in the 260–360 cm^{-1} region using ten Lorentzian components. All the parameters of the Lorentzians are left free in the fitting procedure and the result is a very constant position, within ±1 cm^{-1}, for all the components in the investigated temperature range. These positions are 351.5, 332, 326, 310, 288 and 279 cm^{-1} for C_1 and 340.5, 314, 297 and 276 cm^{-1} for C_2. The results for the two extreme temperatures investigated, 248 and 408 K, are shown in Fig. 3. The integrated intensities of the 332 and 326 cm^{-1} bands of C_1 and of the 340.5 and 297 cm^{-1} bands of C_2 have been used to build the Arrhenius plot of Fig. 4 according to the following expression:

$$\ln[(I_{340} + I_{297})/(I_{332} + I_{326})] = a \ln([C_1]/[C_2]) = b - (\Delta H/RT) \quad (1)$$

DOI: 10.1002/jrs

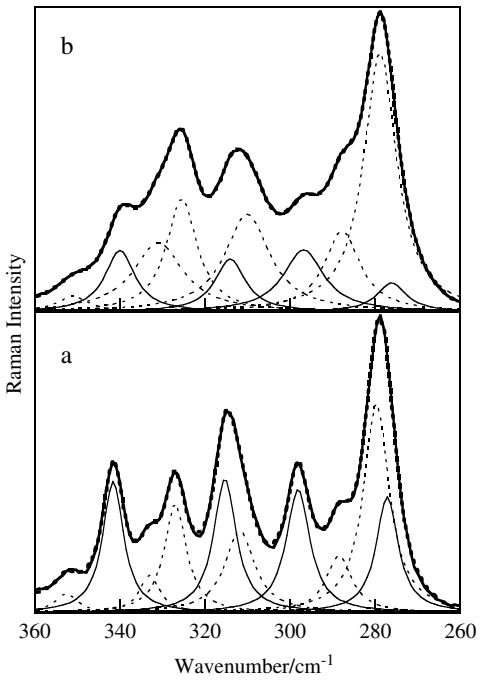

Figure 3. Low-wavenumber Raman spectra of $(EMI^+)TFSI^-$ fitted by ten Lorentzian components: at 248 K (a); and 408 K (b). The C_1 components are shown by the dotted line and the C_2 components by the solid line.

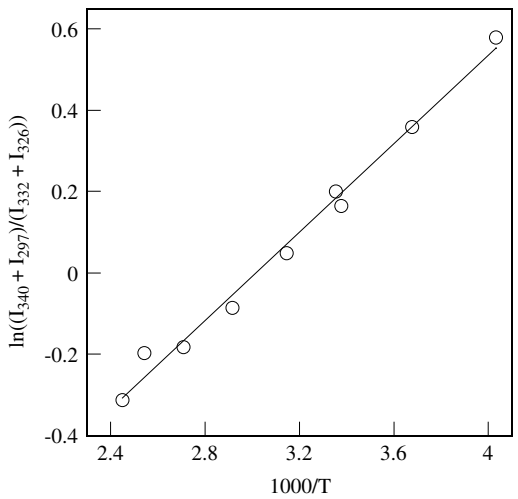

Figure 4. Arrhenius plot in the investigated temperature range of the $(EMI^+)TFSI^-$ ionic liquid using the integrated intensity of the 332 and 326 cm^{-1} anion bands for the C_1 population and the 340 and 297 cm^{-1} anion bands for the C_2 population.

where a and b are constants, $R = 8.3$ J K^{-1} mol^{-1} and T is the absolute temperature. From the slope of the linear variation in Fig. 4, the C_2 conformation is found to be more stable than C_1 by 4.5 ± 0.2 kJ mol^{-1}. By comparison, the calculated gas phase values[2,6] of 2.3–2.9 kJ mol^{-1}, and the experimental value of 2.2 ± 0.5 kJ mol^{-1} previously measured for $TFSI^-$ in a diglyme solution,[8] are significantly smaller; a value of 7 ± 1 kJ mol^{-1} was found[9] in the disordered solid phase of Et_4NTFSI.

The 380–460 cm^{-1} region

Umebayashi *et al*.[1] and Fujii *et al*.[2] have preferred the 380–460 cm^{-1} region for an experimental Raman study of the cation and anion conformations, respectively. Before considering specifically this spectral range, let us comment on the cation conformation in $(EMI^+)Br^-$ at different temperatures (Fig. 5). A comparison of the experimental spectra with those calculated by Umebayashi *et al*.[1] and by us for the np and p conformations of EMI^+ indicates immediately an excellent agreement between the two calculations (Fig. 5(a), (b)). The spectroscopic features of the liquid phase (Fig. 5(c)) are quite similar to those reported in this spectral range for $(EMI^+)BF_4^-$, $(EMI^+)PF_6^-$ and $(EMI^+)CF_3SO_3^-$ by Umebayashi *et al*.,[1] with the advantage for $(EMI^+)Br^-$ to be free of any anion contribution. Umebayashi *et al*. have determined an enthalpy of conformational change of 2–4 kJ mol^{-1} for the cation. Note that the rather intense line of the p conformer calculated at 443.6 cm^{-1} by these authors or at 446.8 cm^{-1} by us (Table 1) is clearly detected in Fig. 5(c). It disappears in the spectrum of solid $(EMI^+)Br^-$ (Fig. 5(d), (e)), as expected by the presence of only an np conformation in the

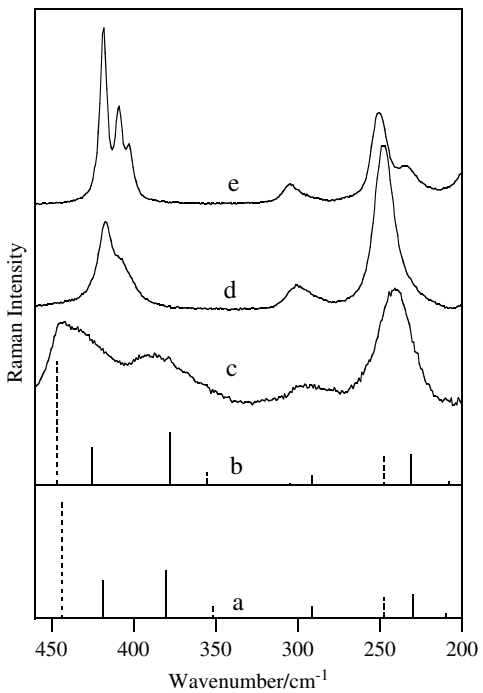

Figure 5. Calculated Raman spectra for the non-planar (solid line) and planar (dotted line) conformers of EMI^+: according to Ref. 1 (a); from Table 1 (b); the experimental spectra of $(EMI^+)Br^-$ liquid at 358 K (c); solid at 298 K (d); and solid at 208 K (e). No scaling factor is applied to the calculated wavenumbers.

DOI: 10.1002/jrs

crystal.[10] The Raman spectra of solid (EMI^+)Br^- (Fig. 5(e), (d)) are then characteristic of the np conformation without any interference from the anion bands. The agreement with the calculated Raman lines is satisfactory, especially near 250 and 300 cm^{-1}. However, some features remain unexplained; e.g. the shoulder at 230 cm^{-1} and the splitting near 400 cm^{-1} are much smaller than predicted. These differences with the calculated gas phase spectrum may come from intermolecular forces that affect more specifically a few vibrations of the solid.

In the 380–460 cm^{-1} region, the (EMI^+)$TFSI^-$ liquid contains contributions from the cation and anion, but the latter are much more intense (Fig. 1). The two available DFT calculations for the anion are again in reasonable agreement (Fig. 6(a), (b)). After scaling, they predict a line of the C_1 conformer at 406 ± 1 cm^{-1} in between two lines of the C_2 conformer at 398 and 413 ± 1 cm^{-1}. The ordered solid phase obtained by slow cooling exhibits the expected intense line at 405.5 cm^{-1} (Fig. 6(c)). Additional peaks at 413 and 426 cm^{-1} may be assigned to vibrations of the EMI^+ np form. The presence of these two peaks might be related to the existence of two families of np cation conformers in the crystal. In the metastable glassy phase, in which nearly all the anions are in the C_2 conformation, two bands are observed at 409 and 398.5 cm^{-1} (Fig. 6(d)). The broad and weak band at ~448 cm^{-1} can be associated with the EMI^+ p conformation. Thus, in the solid ordered phase, the (EMI^+)$TFSI^-$ system stabilizes in a C_1(anion)/np(cation) situation, whereas in the quenched metastable phase it remains in a C_2(anion)/p(cation) conformational state. For a quantitative analysis of this spectral range, Fujii *et al.*[2] used Voigt profiles and fixed positions (three for $TFSI^-$ at 398, 407 and 413 cm^{-1} and four for EMI^+ at 355, 378, 426 and 447 cm^{-1}). They deduce an enthalpy of conformational change of 3.5 kJ mol^{-1}, to be compared to the value of 4.5 kJ mol^{-1} we have determined in the 260–360 cm^{-1} spectral range. Although these values are of the same order of magnitude, their difference is larger than the individual uncertainties. We believe that the 380–460 cm^{-1} region (Fig. 6) is less adequate than the 260–360 cm^{-1} region (Fig. 3) for quantitative measurements. A first obvious reason is the presence of mixed cation and anion contributions in the former region. As noticed in Fig. 6(e–f), the separated lines of the solid state merge into broad profiles in the liquid state. The anion lines are very close and their fitting is highly dependent on the selected band shape.

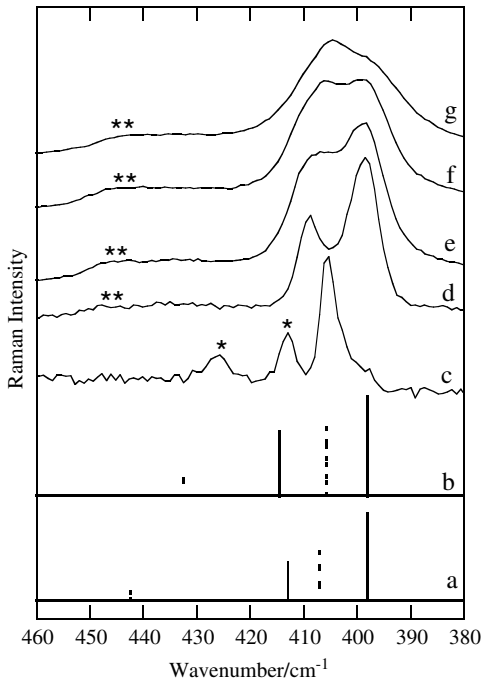

Figure 6. Same as Fig. 2, but in a different spectral range. The single and double asterisks indicate cation contributions due to the non-planar and planar conformers, respectively.

The 730–760 cm^{-1} region

The most intense anion line in the (EMI^+)$TFSI^-$ Raman spectra near 740 cm^{-1} comes from a contraction/expansion of the whole $TFSI^-$ anion.[7,8] According to our DFT calculations, it is predicted at 713.1 cm^{-1} for the C_1 conformer and at 716.1 cm^{-1} for the C_2 conformer.[8] In contrast, Fujii *et al.*[2] find nearly coincident lines for the two conformers at 730.2 and 730.0 cm^{-1}, respectively, from their B3LYP/6-311 + G(3df) calculation. However, their B3LYP/6-31G(d) calculation gives 713.0 and 715.6 cm^{-1}, respectively, i.e. values very similar to ours.

What do the experimental spectra say? We have seen that fast cooling quenches the C_2 form at low temperatures, whereas slow cooling favours the C_1 form. The result of these two cooling processes is a C_2 line at 743.6 cm^{-1} (Fig. 7(a)) and a C_1 line at 740.8 cm^{-1} (Fig. 7(b)). The observed splitting of 2.8 cm^{-1} is quite comparable to our calculated splitting of 3 cm^{-1} and the 2.6 cm^{-1} splitting found by Fujii *et al.*[2] in their B3LYP/6-311 + G(3df) calculation. Therefore, the calculation that gives the best scaling factor for the entire spectrum is not necessarily optimal to reproduce conformational splittings. After scaling, the calculated wavenumbers produce the vertical bars at 744 and 740.1 cm^{-1} represented in Fig. 7. On the basis of this observation, one can more confidently fit the broad and featureless band observed for the liquid state in terms of a conformational equilibrium between the C_1 and C_2 forms. We have used Lorentzian profiles, and the results are illustrated in Fig. 7(c) and (d) for the two extreme temperatures of 248 K and 408 K. The fitted components are separated by about 2 cm^{-1} and the low-wavenumber components become more intense by heating, as expected for a displacement of the equilibrium towards the C_1 form. Any quantitative work in this spectral range would, however, be inaccurate as the result is highly dependent on the chosen band shape.

DOI: 10.1002/jrs

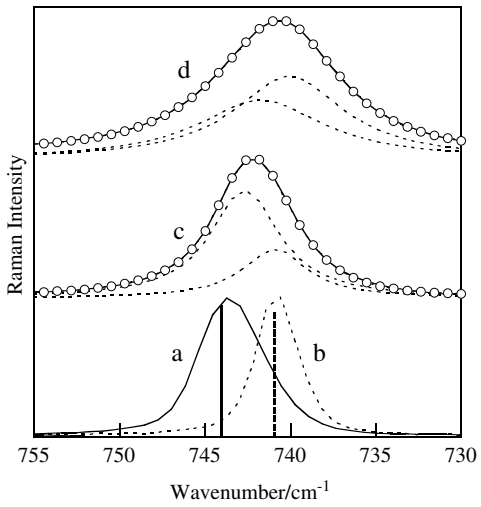

Figure 7. Calculated Raman spectra for the C_2 (solid vertical line) and C_1 (dotted vertical line) $TFSI^-$ conformers using the data reported in Ref. 8 and a scaling factor of 1.039, compared to the experimental spectra of solid $(EMI^+)TFSI^-$: at 113 K obtained by fast cooling (a); by slow cooling (b). The experimental spectra of the liquid phase of $(EMI^+)TFSI^-$: at 248 K (c); and 408 K (d). The latter two spectra (circles) are fitted by two Lorentzian components as explained in the text.

The 1370–1310 cm^{-1} region

The experimental spectra of Fig. 1 show that EMI^+ bands dominate the $(EMI^+)TFSI^-$ spectrum in the 1370–1310 cm^{-1} region, although a doublet coming from the anti-symmetric stretching vibration of the SO_2 groups of $TFSI^-$ is also observed at 1351/1330 cm^{-1}. The two calculations predict measurable conformational splittings for the cation, but there are important differences between the calculated wavenumbers and intensities, as shown in Fig. 8(a) and (b). The experimental spectrum of liquid $(EMI^+)Br^-$ (Fig. 8(d)) confirms the previous observation of an equilibrium between the p and np forms in the liquid state (Fig. 5(c)), although the observed broad band does not reveal the individual contributions. In solid $(EMI^+)Br^-$ (Fig. 8(c)), a much narrower band is observed at ~1340 cm^{-1} in agreement with the calculated line of the np form (Fig. 8(b)). The solid $(EMI^+)TFSI^-$ phase obtained by slow cooling contains a majority of np conformers characterized by the main peak at 1340 cm^{-1} (Fig. 8(e)). The other peaks come in part from the in-phase and out-of-phase anti-symmetric stretching vibrations of the SO_2 groups of $TFSI^-$ at 1353 and 1333 cm^{-1}, respectively, and in part from a possible contribution of cation p conformers giving the weak band at 1357 cm^{-1}. All these bands broaden in liquid $(EMI^+)TFSI^-$ and result in a featureless profile from which the respective contributions of the cation and the anion cannot be extracted (Fig. 8(f)).

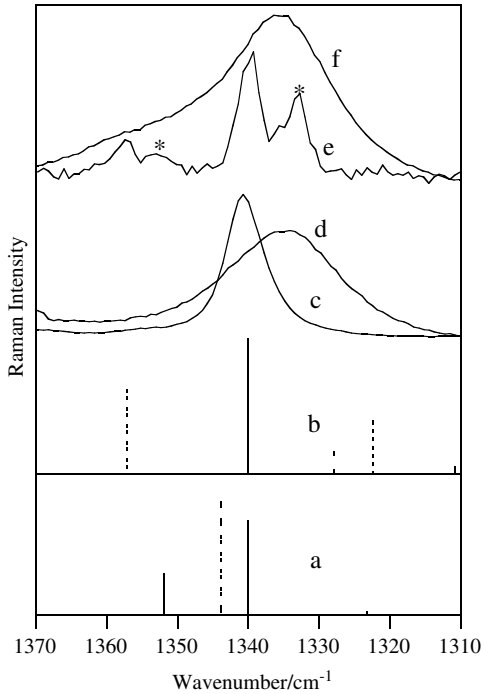

Figure 8. Calculated Raman spectra for the non-planar (solid line) and planar (dotted line) conformers of EMI^+: according to Ref. 1 with a scaling factor of 0.985 (a); according to Table 1 with a scaling factor of 0.995: (b). The experimental spectra of $(EMI^+)Br^-$ solid at 298 K (c); liquid at 358 K (d); $(EMI^+)TFSI^-$ solid at 113 K (slow cooling) (e); liquid at 298 K (f). The scaling factors have been arbitrarily chosen to obtain coincidence with the peak of the non-planar conformer observed in $(EMI^+)TFSI^-$ at 1340 cm^{-1}. Asterisks indicate peaks due to $TFSI^-$ vibrations (see text).

DISCUSSION

DFT calculations

Our DFT calculations on $TFSI^-$ and EMI^+ are in reasonable agreement with those published after,[2] or before,[1] respectively, as illustrated in Figs 2, 5 and 6. The agreement is worse above 450 cm^{-1}. We found for example, a conformational splitting of 3 cm^{-1} for the intense 740 cm^{-1} Raman line (Fig. 7), when no splitting was predicted in another type of calculation.[2] Even more important differences are observed between the two calculations of the EMI^+ lines around 1340 cm^{-1} (Fig. 8). As already pointed out, the best prediction for the entire spectrum does not ensure the best relative sensitivity to structural changes when compared to the experimental reality.

Effect of the anion on the EMI^+ conformation

The EMI^+ liquid salts studied up to now by Raman spectroscopy involve bulky anions, such as[1,2] $TFSI^-$, $CF_3SO_3^-$, BF_4^- or PF_6^-. The similarity of the cation Raman spectra confirms the idea that the EMI^+ conformational state in the liquid phase depends very little on the nature of the

DOI: 10.1002/jrs

anion. Nevertheless, hydrogen-bond interactions between the acidic imidazolium hydrogens and the anion basic centres have been modelled or discussed,[10–16] and one can infer that these interactions are slightly stronger with Br^- than with the other bulky anions. As the energy difference between the two EMI^+ conformers is very small in the gas phase (~2 kJ mol^{-1}), small variations in the cation/anion interactions might induce significant changes of the conformational state in the liquid phase. We found, however, that the Raman spectra, and hence the EMI^+ conformational state, remain very similar when the bulky anions are replaced by Br^-. It is only in the solid (EMI^+)Br^- phase that the cation np form is stabilized, in agreement with the known crystal structure.[10] To detect differences in hydrogen-bonding interactions, it would be necessary to investigate carefully the region of the aromatic CH stretching vibrations.

Population of the anion and cation conformers in (EMI^+)TFSI$^-$

Once vibrations that produce measurable conformational splittings for either the C_1 and C_2 TFSI$^-$ conformers or the p and np EMI^+ conformers have been identified, it becomes possible to evaluate conformer populations. The Raman band intensities I_i are proportional (factor α) to the population n_i of conformer i, to its multiplicity m_i and to the Raman scattering cross-section σ_i of the considered vibration:

$$I_i = \alpha n_i \sigma_i m_i \tag{2}$$

The multiplicities are $m_{C1} = 4$, $m_{C2} = 2$ for the anion and $m_{np} = 2$, $m_p = 1$ for the cation. The quantity of anions in, for example, the C_1 conformation is thus given by:

$$n_{C1}/(n_{C1} + n_{C2}) = I_{C1}/[I_{C1+}2(\sigma_{C1}/\sigma_{C2})I_{C2}] \tag{3}$$

with $n_{C1} + n_{C2} = 1$, and similarly for the quantity of cations in the np conformation:

$$n_{np}/(n_{np} + n_p) = I_{np}/[I_{np+}2(\sigma_{np}/\sigma_p)I_p] \tag{4}$$

with $n_{np} + n_p = 1$. Absolute values of the Raman scattering cross-sections are given here by our *ab initio* calculations. It is well known, however, that these calculated values have to be considered with care. To check their accuracy, comparisons with experimental data are possible. For example, the calculated and experimental intensities can be conveniently compared in cases where a unique conformational state is obtained at low temperature. One can notice in Figs 2 and 6 that the agreement is fair. Another possibility, for the cation, is provided by the (EMI^+)Br^- salt, which has been found to involve only the np conformation in the solid phase.

Using the above criteria, we have tried to evaluate the conformer populations in liquid (EMI^+)TFSI$^-$. For the anion, the data of Fig. 4, i.e. the areas of the 332 and 326 cm^{-1} bands for C_1 and those of the 340 and 297 cm^{-1} bands for C_2, can be exploited. The respective scattering cross-sections of the corresponding vibrations have previously been calculated as 6.5 and 2.6 Å^4 u^{-1} for the 332 and 326 cm^{-1} C_1 bands, respectively, and 3.5 and 3.2 Å^4 u^{-1} for the 340 and 297 cm^{-1} C_2 bands, respectively (Table 1 of Ref. 8). The ratio σ_{C1}/σ_{C2} in Eqn (3) is then $(6.5 + 2.6)/(3.5 + 3.2) = 1.36$. Note that in the calculation of Fujii *et al.*,[2] this ratio is of the same order of magnitude: $(5.5 + 2.09)/(2.6 + 2.19) = 1.58$.

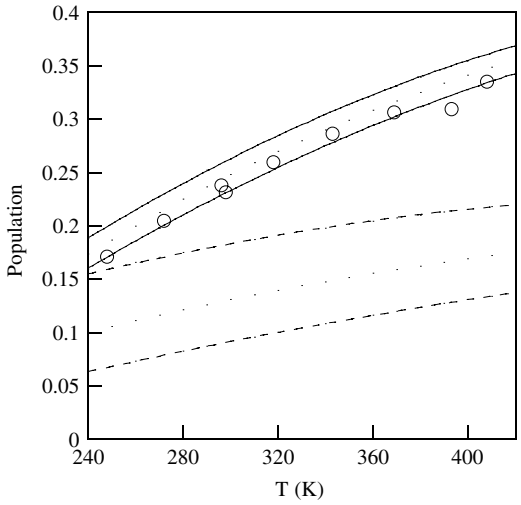

Figure 9. Population of C_1 anion conformers in liquid (EMI^+)TFSI$^-$ evaluated from the $\Delta H = 4.5 \pm 0.2$ kJ mol^{-1} value (in between solid lines) or from the calculated scattering cross-sections (circles, text and Table 1). The population of p EMI^+ conformers (in between dotted lines) is evaluated from the $\Delta H = 3 \pm 1$ kJ mol^{-1} value reported by Umebayashi *et al*.[1]

A straightforward comparison with the experimental data can also be made using the classical expression:

$$n_{C1}/n_{C2} = (m_{C1}/m_{C2}) \exp[-\Delta H_{(C1-C2)}/RT] \tag{5}$$

$\Delta H_{(C1-C2)}$ has previously been evaluated as 4.5 ± 0.2 kJ mol^{-1} (Fig. 4) and $m_{C1}/m_{C2} = 4/2$. It is easy to deduce the percentage of, for example, C_1 conformers as a function of temperature. A similar method can be used for the cation, by plugging in Eqn (6) the Umebayashi *et al*. estimation[1] of 3 ± 1 kJ mol^{-1} for $\Delta H_{(p-np)}$ and $m_p/m_{np} = 1/2$.

$$n_p/n_{np} = (m_p/m_{np}) \exp[-\Delta H_{(p-np)}/RT] \tag{6}$$

The results are summarized in Fig. 9. The different methods to determine the anion C_1 population give consistent results. Large error bars have been associated with the $\Delta H_{(p-np)}$ value for the cation. Nevertheless, one can safely conclude that in (EMI^+)TFSI$^-$ at room temperature the cation adopts mainly the np form ($87 \pm 4\%$) and the anion the C_2 form ($75 \pm 2\%$).

CONCLUSIONS

As already shown with the (Et_4N^+)TFSI$^-$ derivative,[9] and confirmed here with (EMI^+)TFSI$^-$, the conformational state

DOI: 10.1002/jrs

of the $TFSI^-$ anion in ionic liquids can be determined using the complementary information of DFT calculations and Raman spectroscopy. Our results on liquid $(EMI^+)TFSI^-$ are in good agreement with those previously published by Umebayashi *et al*.[1] and by Fujii *et al*.[2] Complementary information is provided in the present work, using for example, a method that consists in solidifying the ionic liquids either quickly to obtain a quenched metastable phase or slowly to obtain an ordered solid phase. The conformational equilibrium of the liquid phase can thus be displaced towards unique conformational states, and well-defined Raman spectra are obtained that can efficiently be compared with the calculated spectra. This concept applies also to the cations. $(EMI^+)Br^-$ is an interesting reference salt since its crystal structure has been determined and its Raman spectrum contain only the cation lines. However, the thermal history has to be considered with care. Large differences are noted between the melting temperature measured by heating and the solidification temperature measured by cooling.[22] They are, for example, reported as 352 and 303 K, respectively, for $(EMI^+)Br^-$ and as 257 and 223 K, respectively, for $(EMI^+)TFSI^-$.[22] The melting temperature of the purchased $(EMI^+)Br^-$ (99+%) was claimed[17] to be 326 K, but during the Raman experiments, we found that $(EMI^+)Br^-$ was still solid at 343 K and was liquefied only by heating above 352 K. The cooling rate of the liquid phase also has a great influence on the nature of the solid phase. Fast cooling of liquid $(EMI^+)TFSI^-$ quenches a metastable glass phase characterized by a C_2(anion)/p(cation) conformational state, whereas slow cooling leads to a crystalline phase characterized by a C_1(anion)/np(cation) conformational state. We have just been made aware of a differential scanning calorimetry (DSC) and X-ray diffraction study of $(EMI^+)TFSI^-$ by Choudhury *et al*.,[23] in which the melting temperature, measured by heating, is shown to be 247.3 K and the crystal (non-centrosymmetric space group $Pca2_1$, $Z = 2$) is confirmed to be composed of C_1 anions and of np cations.

Quantitative measurements performed over a wide temperature range of the $(EMI^+)TFSI^-$ ionic liquid and in the 260–360 cm^{-1} Raman region show that the C_2 anion conformer is more stable than C_1 one by 4.5 kJ mol^{-1}, which may be compared with 2–3 kJ mol^{-1} in the gas phase or in dilute solutions of non-polar solvents. At room temperature, the population of the C_2 anion conformers and np cation conformers is $(75 \pm 2\%)$ and $(87 \pm 4\%)$, respectively.

Acknowledgements

The authors are grateful to David Talaga for his experimental support and to Wesley A. Henderson for stimulating discussions. One of us (R.H.) acknowledges the scholarship from the Swedish Institute for this project. The financial support from the Swedish Research Council and the FUTURA foundation, and the computer time provided by SNAC, are gratefully acknowledged.

REFERENCES

1. Umebayashi Y, Fujimori T, Sukizaki T, Asada M, Fujii K, Kanzaki R, Ishiguro S-I. *J. Phys. Chem. A* 2005; **109**: 8976.
2. Fujii K, Fujimori T, Takamuku T, Kanzaki R, Umebayashi Y, Ishiguro S-I. *J. Phys. Chem. B* 2006; **110**: 8179.
3. Noda A, Hayamizu K, Watanabe M. *J. Phys. Chem. B* 2001; **105**: 4603.
4. Garcia B, Lavallée S, Perron G, Michot C, Armand M. *Electrochim. Acta* 2004; **49**: 4583.
5. Tokuda H, Hayamizu K, Ishii K, Susan ABH, Watanabe M. *J. Phys. Chem. B* 2005; **109**: 6103.
6. Johansson P, Gejji SP, Tegenfeldt J, Lindgren J. *Electrochim. Acta* 1998; **43**: 1375.
7. Rey I, Johansson P, Lindgren J, Lassègues JC, Grondin J, Servant L. *J. Phys. Chem. A* 1998; **102**: 3249.
8. Herstedt M, Smirnov M, Johansson P, Chami M, Grondin J, Servant L, Lassègues JC. *J. Raman Spectrosc.* 2005; **36**: 762.
9. Herstedt M, Henderson WA, Smirnov M, Ducasse L, Servant L, Talaga D, Lassègues JC. *J. Mol. Struct.* 2006; **783**: 145.
10. Elaiwi A, Hitchcock PB, Seddon KR, Srinivasan N, Tan YM, Welton T, Zora JA. *J. Chem. Soc., Dalton Trans.* 1995; 3467.
11. Turner EA, Pye CC, Singer RD. *J. Phys. Chem. A* 2003; **107**: 2277.
12. Talaty ER, Raja S, Storhaug VJ, Dölle A, Carper WR. *J. Phys. Chem. B* 2004; **108**: 13177.
13. Canongia Lopes JN, Deschamps J, Pádua AAH. *J. Phys. Chem. B* 2004; **108**: 2038.
14. Del Pópolo MG, Voth GA. *J. Phys. Chem. B* 2004; **108**: 1744.
15. Liu Z, Huang S, Wang W. *J. Phys. Chem. B* 2004; **108**: 12978.
16. Tsuzuki S, Tokuda H, Hayamizu K, Watanabe M. *J. Phys. Chem. B* 2005; **109**: 16474.
17. http://www.solvionic.com [2006].
18. Frisch MJ, Trucks GW, Schlegel HB, Scuseria GE, Robb MA, Cheeseman JR, Montgomery JA Jr, Vreven T, Kudin KN, Burant JC, Millam JM, Iyengar SS, Tomasi J, Barone V, Mennucci B, Cossi M, Scalmani G, Rega N, Petersson GA, Nakatsuji H, Hada M, Ehara M, Toyota K, Fukuda R, Hasegawa J, Ishida M, Nakajima T, Honda Y, Kitao O, Nakai H, Klene M, Li X, Knox JE, Hratchian HP, Cross JB, Bakken V, Adamo C, Jaramillo J, Gomperts R, Stratmann RE, Yazyev O, Austin AJ, Cammi R, Pomelli C, Ochterski JW, Ayala PY, Morokuma K, Voth GA, Salvador P, Dannenberg JJ, Zakrzewski VG, Dapprich S, Daniels AD, Strain MC, Farkas O, Malick DK, Rabuck AD, Raghavachari K, Foresman JB, Ortiz JV, Cui Q, Baboul AG, Clifford S, Cioslowski J, Stefanov BB, Liu G, Liashenko A, Piskorz P, Komaromi I, Martin RL, Fox DJ, Keith T, Al-Laham MA, Peng CY, Nanayakkara A, Challacombe M, Gill PMW, Johnson B, Chen W, Wong MW, Gonzalez C, Pople JA. *Gaussian 03, Revision C.02*. Gaussian, Inc: Wallingford, 2004.
19. Lee C, Yang W, Parr RG. *Phys. Rev., B* 1988; **37**: 785.
20. Becke AD. *J. Chem. Phys.* 1993; **98**: 5648.
21. Vosko SH, Wilk L, Nusair M. *Can. J. Phys.* 1980; **58**: 1200.
22. Galiński M, Lewandowski A, Stępniak I. *Electrochim. Acta* 2006; **51**: 5567.
23. Choudhury AR, Winterton N, Steiner A, Cooper AI, Johnson KA. *Cryst. Eng. Commun.* 2006; **8**: 742.

DOI: 10.1002/jrs